Journal of Engineering Physics and Thermophysics, Vol. 66, No. 5, 1994

NUMERICAL MODELING OF LIGHT-INDUCED CONVECTION AND THERMOOPTICAL INTERACTION OF A VERTICAL RADIATION BEAM WITH LIQUIDS

N. Ye. Galich and V. A. Petrushchenkov

UDC 535.2:621.378.8

Dimensional analysis, results of numerical modeling of nonlinear thermooptical interaction of a vertical radiation beam with liquids in a vertical cylinder in the presence of light-induced convection, and their comparison with available experiments are given.

1. Light-induced convection due to the heating of a medium by absorption of a portion of the energy of radiation that propagates in a liquid or a gas manifests itself in transportation of laser radiation energy, in optical pyrolysis, and in photochemical processes and has a pronounced effect on the intensity distribution and the divergence and coherence of a light beam. Nonlinear interference of radiation and convection is associated with a temperature dependence of the refractive index or the dielectric permittivity of the medium $\varepsilon(T)$, the radiation beam forming a nonlinear lenticular medium. In most weakly absorbing media $\varepsilon_T = d\varepsilon/dT < 0$, which leads to thermal self-defocusing of radiation. The indicated processes manifest themselves at a very moderate radiation power, which makes for their study and consideration in propagation of radiation under laboratory, industrial, and natural conditions a practical necessity.

Problems of convection induced by a horizontal radiation beam have received rather thorough study. In a vertical beam convection of a liquid along the beam causes a far more complex and diverse picture of the effects of thermooptical interaction. Experiments [1, 2] show that none of the earlier theoretical solutions [3–11] yields a satisfactory description of the observed phenomena. Approximating the boundary layer within the framework of a self-consistent thermohydrooptical problem [12, 13] enables us to understand and determine the basic features of steady-state convection and self-defocusing in an unbounded medium. An analytical description of steady-state convection in a bounded cavity [14] involves approximating [5] the convection relation and introducing additional semiempirical functional dependences that characterize self-defocusing of radiation. The present work is oriented to a numerical solution of a combined system of convection equations in the Boussinesq approximation and those of radiation propagation in the small-angle approximation (the quasioptical approximation), which enables us to perform successive analysis of both the stationary and nonstationary phases of thermooptical interaction of radiation with liquids, obtain and substantiate a series of correlation dependences, and explain the nature and cause of the effects observed in experiments [1, 2]. Numerical modeling is limited to laminar regimes of convection. Criteria and thesholds of generation of turbulence are given in [15].

2. We consider axisymmetric light-induced flow in a vertical cylinder of finite height H, $\overline{H} = H/\Lambda_0$, $\overline{R} = R/\Lambda_0$, and of radius R, and the vertical coincides with the z axis, $\overline{z} = z/\Lambda_0$, $\overline{r} = r/\Lambda_0$. The equations of motion for the dimensionless vertical $\overline{u} = u\Lambda_0/\nu$ and horizontal $\overline{v} = v\Lambda_0/\nu$ velocity components have the form

$$\partial_{\overline{t}}\,\overline{u} + \overline{u}\,\partial_{\overline{z}}\,\overline{u} + \overline{v}\,\partial_{\overline{r}}\,\overline{u} = -\partial_{\overline{z}}\,\overline{p} + \Delta_{\perp}\overline{u} + \partial^2_{\overline{z}\,\overline{z}}\,\overline{u} + \mathrm{Gr}\,\overline{T}\,, \quad \Delta_{\perp} = \overline{r}^{-1}\,\partial_{\overline{r}}\,(\overline{r}\,\partial_{\overline{r}})\,, \tag{1}$$

$$\partial_{\overline{t}}\,\overline{v} + \overline{u}\,\partial_{\overline{z}}\,\overline{v} + \overline{v}\,\partial_{\overline{r}}\,\overline{v} = -\partial_{\overline{r}}\,\overline{p} + \Delta_{\perp}\overline{v} + \partial^2_{\overline{z}\,\overline{z}}\,\overline{v} - \overline{v}\,\overline{r}^{-2}\,. \tag{2}$$

St. Petersburg State Technical University. Translated from Inzhenerno-Fizicheskii Zhurnal, Vol. 66, No. 5, pp. 547-555, May, 1994. Original article submitted December 8, 1992.

1062-0125/94/6605-0481$12.50

The bar denotes the dimensionless variables $\bar{t} = t\nu/\Lambda_0^2$, i.e., the time, $\bar{p} = p\Lambda_0^2/\rho\nu^2$, i.e., the pressure, $\bar{T} = T\kappa/\alpha I_0\Lambda_0^2$, i.e., the temperature excess with respect to the temperature of the isothermal boundaries of the cylindrical cavity; Λ_0 is the initial width of the radiation beam at the inlet to the liquid; I_0 is the initial radiation intensity on the beam axis. The heat-conduction and continuity equations have the form

$$\partial_{\bar{t}}\bar{T} + \bar{u}\,\partial_{\bar{z}}\bar{T} + \bar{v}\,\partial_{\bar{r}}\bar{T} = \mathrm{Pr}^{-1}(\Delta_{\perp}\bar{T} + \partial^2_{\bar{z}\bar{z}}\bar{T}) + \bar{I}, \tag{3}$$

$$\partial_{\bar{z}}(\bar{u}\bar{r}) + \partial_{\bar{r}}(\bar{v}\bar{r}) = 0. \tag{4}$$

The heat source in (3) due to Bouguer absorption of radiation is determined by radiation transfer equations in the intensity I–eikonal s variables [4, 12–15]:

$$\partial_{\bar{z}}\bar{I} + \bar{r}^{-1}\,\partial_{\bar{r}}(\bar{I}\,\partial_{\bar{r}}\bar{s}\,\bar{r}) + \bar{\alpha}\bar{I} = 0, \quad \bar{\alpha} = \alpha\Lambda_0, \quad \bar{k} = k\Lambda_0, \tag{5}$$

$$2\partial_{\bar{z}}\bar{s} + (\partial_{\bar{r}}\bar{s})^2 = \bar{\varepsilon}_{\mathrm{T}}\bar{T} + \Delta_{\perp}\bar{I}^{1/2}/\bar{k}^2\bar{I}^{1/2}, \quad \bar{\varepsilon}_{\mathrm{T}} = \varepsilon_{\mathrm{T}}\alpha I_0\Lambda_0^2/\varepsilon_0\kappa, \tag{6}$$

where $\bar{I} = I/I_0$, $\bar{s} = s/\Lambda_0$, $\varepsilon_0 = \varepsilon(I = 0)$, k is the wave vector of radiation; the first and the second terms in the right-hand side of (6) characterize nonlinear refraction (self-defocusing) and diffraction divergence of the radiation beam.

3. Dimensional analysis of system of equations (1)–(3) was performed by a standard procedure (see, for example, [3] as well as [8, 9]). Analyzing the complete system of equations (1)–(6) by the same procedure showed a substantial effect of radiation self-defocusing. All possible combinations of convection regimes with "weak" and "strong" self-defocusing of radiation were considered. The self-defocusing was assumed "strong" when the terms in the left-hand side of (5) are commensurable; $\partial_{\bar{r}}\bar{s} \sim \bar{w}/\bar{H}$, $\bar{w} = w/\Lambda_0$. As numerical results showed, this condition is satisfied for $\bar{w} \gtrsim 1.1$. Otherwise, for $\bar{w} \lesssim 1.1$, self-defocusing of radiation is "weak" and can be disregarded by considering the approximation of the prescribed (and constant) radiation intensity within the framework of (1)–(3). Tables 1 and 2 give results of dimensional analysis using estimates of characteristic values of temperature T and velocity u on the beam axis, beam width w, and time τ in which the process of thermooptical interaction of the beam with the liquid in the cell is established. The regime boundaries between "weak" and "moderate" convection were defined by the conditions $\mathrm{Gr} \sim \overline{HR}^{-6}\mathrm{Pr}^{-2}$ ($\mathrm{Pr} \gg 1$), $\mathrm{Gr} \sim \overline{HR}^{-6}\mathrm{Pr}^{-1}$ ($\mathrm{Pr} \ll 1$) and those between "moderate" and "developed" convection were defined by $\mathrm{Gr} \sim \overline{HR}^{-6}$ ($\mathrm{Pr} \gg 1$), $\mathrm{Gr} \sim \overline{HR}^{-6}\mathrm{Pr}^{-3}\mathrm{Pr} \ll 1$. The terms "weak," "moderate," and "developed" convection, like the classification of the corresponding regimes of convection, were proposed in [8]. It is noteworthy that the regime of "developed" convection corresponds to turbulent flow [15] and the regimes of "weak" and "moderate" convection correspond to laminar flow. The natural limitation $\Lambda_0 \lesssim R$ is also noteworthy. To estimate the average-over-the beam intensity $\tilde{I}$ averaged over the cross section, we need only take into account the definition of the average width $w^2 = \int_0^R Ir^3dr / \int_0^R Irdr$ and the presence of the integral $P = 2\pi\int_0^R Irdr = P_0\exp(-\alpha z)$, which is a consequence of (6), or the condition $I_0w_0^2 = \tilde{I}w^2$. The given relations for temperature and velocity in the case of "weak" convection are in agreement with the results of the analysis [5, 8]. The estimate of the average width of the radiation beam w in [16] takes no account of convective heat transfer along the beam and therefore is at variance with the results given in Table 1 as well as with those of experiments [1, 2].

4. System of equations (1)–(6) was solved numerically by the method of establishment with the choice of the following iteration procedure. Velocity and temperature fields were determined from the radiation intensity known at the previous time step. The radiation intensity at the current time step was found from the temperature

TABLE 1. Estimate of T, u, and w for "Weak" Self-Defocusing

Regimes	Temperature T	Velocity u
"Weak" convection	$\frac{\alpha I_0 \Lambda_0^2 \mathrm{Pr}}{\kappa} \exp(-\alpha H)$	$\frac{g\beta\alpha I_0 \Lambda_0^2 R^2}{\mathrm{Pr}\,\kappa\chi} \exp(-\alpha H)$
"Moderate" convection Pr >> 1	$\left(\frac{I_0 \chi \mathrm{Pr}^3 (1-\exp(-\alpha H))}{\rho C_p g\beta \Lambda_0^2}\right)^{1/2}$	$\left(\frac{g\beta I_0 R^4 (1-\exp(-\alpha H))}{\Lambda_0^2 \kappa \mathrm{Pr}}\right)^{1/2}$
"Moderate" convection Pr $\lesssim$ 1	$\frac{\alpha I_0 \Lambda_0^2 \mathrm{Pr}}{\kappa} \exp(-\alpha H)$	$\left(\frac{g\beta\alpha I_0 \Lambda_0^2 H}{\kappa} \exp(-\alpha H)\right)^{1/2}$
"Developed" convection	$\left(\frac{I_0^2 (1-\exp(-\alpha H))^2 \mathrm{Pr}^3}{\rho^2 C_p^2 g\beta H}\right)^{1/3}$	$\left(\frac{g\beta I_0 H (1-\exp(-\alpha H))}{\rho C_p}\right)^{1/3}$
Regimes	Widening of the beam $w-\Lambda_0$	Time for estblishment τ
"Weak" convection	$\frac{\lvert\varepsilon_T\rvert H^3 \chi^2 \exp(\alpha H) \mathrm{Pr}^2}{\Lambda_0^3 \varepsilon_0 g\beta R^2}$	$\frac{\Lambda_0^2}{\chi}$
"Moderate" convection Pr >> 1	$\left(\frac{I_0 \alpha^2 \varepsilon_T^2 \chi H^6 \mathrm{Pr}^3}{\rho C_p \varepsilon_0^2 g\beta R^4 (1-\exp(-\alpha H))}\right)^{1/2}$	$\left(\frac{H^2 \Lambda_0^2 \kappa \mathrm{Pr}}{g\beta I_0 R^4 (1-\exp(-\alpha H))}\right)^{1/2}$
"Moderate" convection Pr $\lesssim$ 1	$\left(\frac{I_0 \alpha \varepsilon_T^2 \chi H^5 \mathrm{Pr}^2 \exp(\alpha H)}{\varepsilon_0^2 \rho C_p g\beta \Lambda_0^4}\right)^{1/2}$	$\frac{\Lambda_0^2}{\chi}$
"Developed" convection	$\left(\frac{I_0^2 \alpha^3 \lvert\varepsilon_T\rvert^3 \chi H^8 \mathrm{Pr}^3}{\Lambda_0^3 \varepsilon_0^3 \rho C_p g\beta (1-\exp(-\alpha H))}\right)^{1/3}$	$\left(\frac{H^2 \rho C_p}{g\beta I_0 (1-\exp(-\alpha H))}\right)^{1/3}$

field as a first iteration approximation. The velocity and temperature fields were then corrected and so on until the intensity ceased to change, accurate to within 0.1%.

To solve the system of convection equations (1)– (4), we chose a multistep finite-difference method, employing an implicit conservative approximation scheme [17]. The radiation propagation equations (5) and (6) were approximated by an explicit conservative three-layer scheme with stepping over ("leap-frog").

The motion of the medium was calculated, as a rule, on a nonuniform 20 × 20 grid and in individual cases on a 40 × 40 grid, which ensured sufficient accuracy for the results [10]. Division along the radial and axial coordinates was realized using transforming logarithmic and exponential functions that ensured compression of the grid in the vicinity of the axis and in the direction of radiation propagation. For the radiation beam the grid was formed as follows. Nodes along the radial coordinate were found as a result of uniform division of the cell radius. Nodes along the axial coordinate were obtained as a result of uniform division of the grid steps used in calculating convection into 8 parts. In connection with the unequally divided calculation region in solving the hydrodynamic problem and the thermooptics problem the equations of convection and radiation transfer were joined using linear interpolation of the temperature field. As a rule, in calculating radiation use was made of a 75 × 153 grid. Control of convergence of the calculations was ensured by preserving the integral of radiation power $P = 2\pi \int_0^R Irdr = P_0(\exp(-\alpha z)$ with an error of no more than 2%. The use of a conservative scheme also implied automatic fulfillment of the condition $\int_0^R urdr = 0$. Thus, fulfillment of all local and integral conservation laws was ensured.

TABLE 2. Estimation of T, u, w, and τ for "Strong" Self-Defocusing

Regimes	Temperature T	Velocity u
"Weak" convection	$\frac{\alpha I_0 \Lambda_0^2}{\kappa} \mathrm{Pr} \exp(-\alpha H)$	$\frac{g\beta\alpha I_0 \Lambda_0^2 R^2}{\mathrm{Pr}\kappa\chi} \exp(-\alpha H)$
"Moderate" convection Pr >> 1	$\left(\frac{I_0 \Lambda_0^2 \chi \varepsilon_0 \mathrm{Pr}^3 (1-\exp(-\alpha H))}{\rho C_p g\beta \lvert\varepsilon_T\rvert H^2 R^2}\right)^{1/3}$	$\left(\frac{g^2\beta^2 I_0 \Lambda_0^2 \varepsilon_0 R^4 (1-\exp(-\alpha H))}{\rho C_p \lvert\varepsilon_T\rvert \chi^2 H^2 \mathrm{Pr}^3}\right)^{1/3}$
"Moderate" convection Pr $\lesssim$ 1	$\frac{\alpha I_0 \Lambda_0^2}{\kappa} \mathrm{Pr} \exp(-\alpha H)$	$\left(\frac{g\beta\alpha I_0 \Lambda_0^2 H}{\mathrm{Pr}\kappa \exp(\alpha H)}\right)^{1/2}$
"Developed" convection	$\left(\frac{I_0^2 \Lambda_0^4 \varepsilon_0^2 \mathrm{Pr}^3 (1-\exp(-\alpha H))^2}{\rho^2 C_p^2 \varepsilon_T^2 g\beta H^5}\right)^{1/5}$	$\left(\frac{g^2\beta^2 I_0 \Lambda_0^2 \varepsilon_0 (1-\exp(-\alpha H))}{\lvert\varepsilon_T\rvert \rho C_p \mathrm{Pr}}\right)^{1/5}$
Regimes	**Widening of the beam $w-\Lambda_0$**	**Time for establishment τ**
"Weak" convection	$\left(\frac{\alpha I_0 \Lambda_0^2 \lvert\varepsilon_T\rvert H^2 \mathrm{Pr}}{\varepsilon_0 \kappa \exp(\alpha H)}\right)^{1/2}$	$\frac{\alpha I_0 \Lambda_0^2 \lvert\varepsilon_T\rvert H^2 \mathrm{Pr}}{\chi\kappa \exp(\alpha H)}$
"Moderate" convection Pr >> 1	$\left(\frac{I_0 \Lambda_0^2 \varepsilon_T^2 H^4 \mathrm{Pr}^2 (1-\exp(-\alpha H))}{\varepsilon_0^2 \rho C_p g\beta R^2}\right)^{1/6}$	$\left(\frac{\lvert\varepsilon_T\rvert \kappa\chi H^5 \mathrm{Pr}^3}{g^2\beta^2 I_0 \Lambda_0^2 \varepsilon_0 R^4 (1-\exp(-\alpha H))}\right)^{1/3}$
"Moderate" convection Pr $\lesssim$ 1	$\left(\frac{\alpha I_0 \Lambda_0^2 \lvert\varepsilon_T\rvert H^2 \mathrm{Pr}}{\varepsilon_0 \kappa \exp(\alpha H)}\right)^{1/2}$	$\frac{\alpha I_0 \Lambda_0^2 \lvert\varepsilon_T\rvert H^2 \mathrm{Pr}}{\chi\kappa\varepsilon_0 \exp(\alpha H)}$
"Developed" convection	$\left(\frac{I_0^2 \Lambda_0^2 \lvert\varepsilon_T\rvert^3 H^5 \mathrm{Pr}^3 (1-\exp(-\alpha H))^2}{\varepsilon_0^3 \rho^2 C_p^2 g\beta}\right)^{1/10}$	$\left(\frac{\lvert\varepsilon_T\rvert H^5 \rho C_p \mathrm{Pr}}{I_0 \Lambda_0^2 \varepsilon_0 g^2\beta^2 (1-\exp(-\alpha H))}\right)^{1/5}$

We considered different boundary condition. Either the entire cell surface was assumed isothermal or only the lower and lateral surfaces of the cell were assumed isothermal with adiabatic thermal insulation of the upper surface. The rate of convective motion was assumed equal to zero on the cell walls. We analyzed separately the case of a free upper surface of the liquid under the condition that there are no tangential frictional stresses on the free surface, which was assumed flat. Two variants of the direction of radiation propagation were considered, namely, from the bottom upward and from the top downward. The wave front (the eikonal) at the inlet of the radiation beam to the medium corresponded to either a collimated beam or a weak initial divergence of $\sim 10^{-3} - 10^{-2}$ rad. The initial divergence was taken into account by the relation $\bar{s} = \bar{r}^2 \exp(-\bar{r}^2)/2\bar{F}$, F is the radius of the initial divergence of the radiation beam, $\bar{F} = F/\Lambda_0$. The eikonal on vertical walls of the cell was taken equal to zero since we considered the case $\Lambda_0/R \ll 1$ and w/R did not exceed 0.6 in all the investigated situations. At the inlet to the medium the radiation beam was considered Gaussian with the initial intensity profile $\bar{I} = \exp(-\bar{r}^2)$. In the finite-difference approximation for Eqs. (1)–(3), (5), and (6) it was considered that $\Delta_\perp = 2\partial^2_{\bar{r}\bar{r}}$ on the beam axis. Numerical values of the parameters were oriented basically to the conditions of experiments [1, 2], where propagation of a radiation beam with the wavelength 1.06 μm was investigated in various silicon organic liquids. In the present work data of a numerical analysis are presented that refer to just two liquids: polyethyl siloxane with $\nu = 4.5 \cdot 10^{-5}$ m^2/sec (PES-4) and polymethyl siloxane with $\nu = 20$ mm^2/sec (PMS-20) in a cell of height $H = 0.18$ m, with beam width $\Lambda_0 = 3$ mm. For PMS-20 the numerical values of the parameters are $\varepsilon_0 = 1.96$, $\varepsilon_T =$

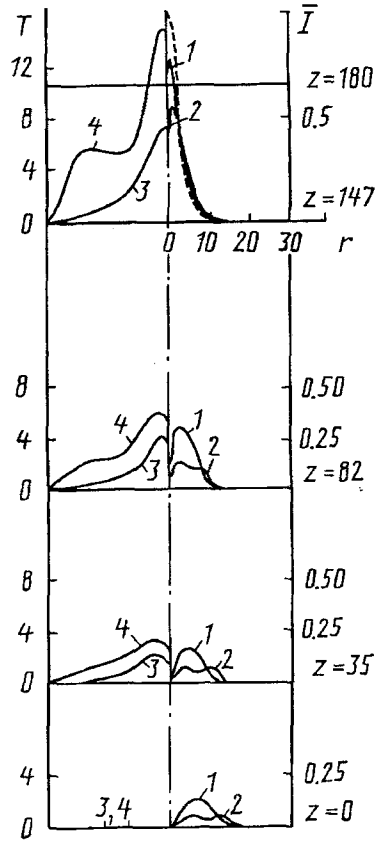

Fig. 1. Radiation intensity and temperature distributions in different cross sections of the calculation region for the counterflow (the beam propagates from the top downward): 1) $\bar{I}$ for PMS-20, $\alpha H = 0.35$, $P_0 = 0.74$ W, $T_н = 0$; 2) $\bar{I}$ for PES-4, $\alpha H = 1$, $P_0 = 74$ W, $\partial_z T|_н = 0$; 3) T for PMS-20; 4) T for PES-4; the dashed line shows the initial Gaussian intensity distribution. T, K; r, z, mm.

$-1.48 \cdot 10^{-3}$ K^{-1}, $\alpha = 1.97$ m^{-1}, Pr = 234, $\rho = 940$ kg/m^3, $C_p = 1717$ J/(kg·K), $\beta = 9.7 \cdot 10^{-4}$ K^{-1}; for PES-4; $\varepsilon_0 = 2.07$, $\varepsilon_T = -1.41 \cdot 10^{-3}$ K^{-1}, $\alpha = 5.94$ m^{-1}, $\rho = 1100$ kg/m^3, $C_p = 1860$ J/(kg·K), $\beta = 7.3 \cdot 10^{-4}$ K^{-1}, Pr = 627. The range of change of the beam power P_0 varied from 13 to 74 W in typical cases. The Fresnel number $N_F = k\Lambda_0^2/H = 314$. The cell cross section was rectangular and had the dimensions 60 × 50 mm in the experiments. In the numerical calculations we considered that $R = 30$ mm, based on the equivalence of the area $\pi R^2 = 50 \times 60$ mm.

Numerical modeling, a small portion of whose results is given in [18], showed that no matter what the value of the parameters of the thermooptical interaction a vortex (toroidal) structure of the flow and a more or less pronounced annular structure of the radiation beam that passed through the liquid are typical (see Fig. 1 in [18] and Fig. 1 of the present work). The annular structure of the radiation beam is caused by convective thermal self-defocusing. Heat transfer by convection along the beam interferes with temperature equalization by heat conduction in the traverse direction. Therefore on the beam axis a temperature maximum or an optical density maximum ($\varepsilon_T < 0$) forms, which leads to self-defocusing of axial rays. Self-defocusing of axial rays is possible, in turn, in an annular beam, which is observed in a liquid with $\alpha H \gg 1$ (Fig. 1). Such a situation also characterizes forced flow of a medium along a ray [12, 13, 19].

Unlike the approximation of a the prescribed intensity, taking account of self-defocusing alters the character and dynamics of establishment of the temperature, velocity, and intensity, depending on the direction of propagation of the radiation beam: from the bottom upward (the cocurrent flow) or from the top downward (the counterflow). In the counterflow there is feedback of the disturbances of T and I at the inlet to the medium and at the outlet from the medium due to self-defocusing and removal of heat by convection toward the oncoming radiation, but there is no such feedback in the cocurrent flow. Figure 2 shows characteristic features of establishment of the

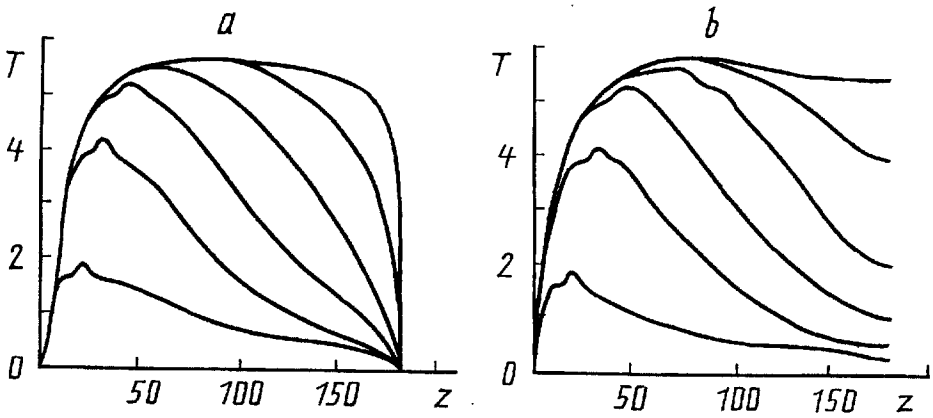

Fig. 2. Temperature distribution on the radiation beam axis in the process of establishment under different thermal conditions on the upper boundary of PMS-20 liquid, the cocurrent flow, with the time step $\Delta t = \pi/6$: a) $T_н = 0$; b) $\partial_z T|_н = 0$.

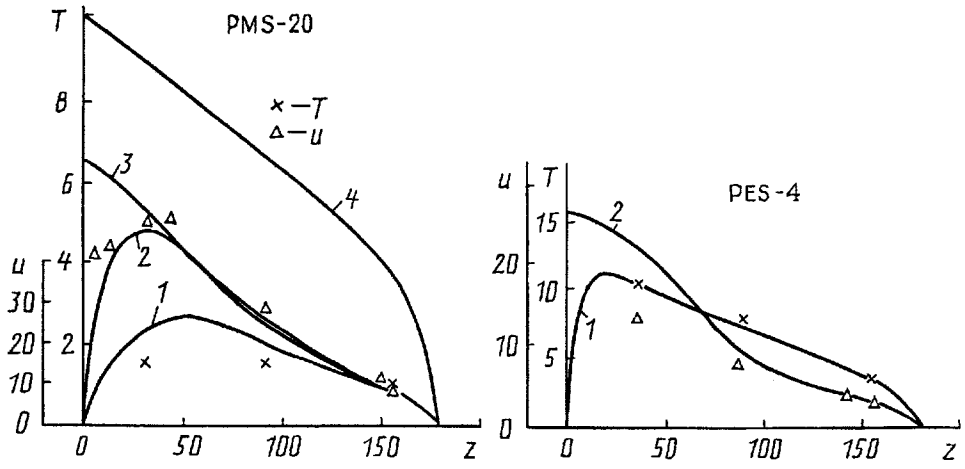

Fig. 3. Steady-state distributions of temperature and velocity on the radiation beam axis for the counterflow: 1) velocity distribution at $T_н = 0$; 2) temperature distribution at $T_н = 0$; 3) temperature distribution at $\partial_z T|_н = 0$; 4) temperature distribution in the approximation of a prescribed intensity; the points are experimental values. u, mm/sec.

temperature in the cocurrent flow. In the cocurrent flow, unlike the counterflow, an establishment wave forms. This fact is in agreement with the observed supernatant heat "bubble" in the liquid in visualization of thermooptical interaction in experiments [1, 2]. In the counterflow the features of establishment of convection and self-defocusing depend on the radiation power level (the values of Gr and $\bar{\varepsilon}_T$) (see Fig. 2 in [18]). With $\mathrm{Gr} \lesssim 0.16$ a steady-state regime is reached in a practically monotonic aperiodic manner. With $\mathrm{Gr} > 0.16$ we observe damped auto-oscillations of the intensity and temperature that are localized in the vicinity of the beam axis. The auto-oscillations are caused by nonlocal feedback of the disturbances of $T(z \to H)$ and $I(z \to 0)$ that is formed in the counterflow through self-defocusing of radiation. More detailed calculations showed that in relatively low-viscosity liquids with $\nu \lesssim 10^{-5}$ m^2/sec the existence of oscillation regimes is also possible in the establishment of the velocity, in full conformity with results of experiments [1, 2].

Analyzing the results of the numerical modeling showed that the time for establishing light-induced convection with acciunt for self-defocusing $\tau \sim I_0^{-0.31} \sim \mathrm{Gr}^{-0.31}$ is larger than the time for establishing convection in the approximation of a prescribed intensity, when the problem reduces to (1) –(3) and $\tau \sim I_0^{-0.5} \sim \mathrm{Gr}^{0.5}$.

Figure 3 compares calculated steady-state distributions of velocity and temperature on the beam axis with experiment [1, 2]. Some deviation of the calculated data from the experimental data is associated with substituting

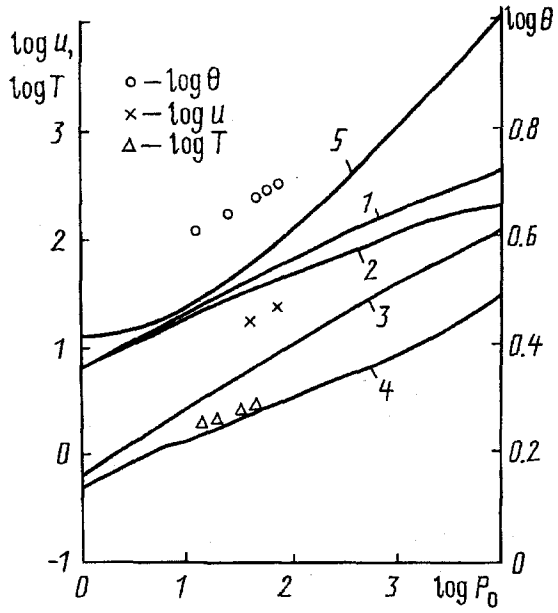

Fig. 4. Velocity, temperature, and divergence of the beam vs. radiation power for the counterflow (PMS-20) in steady-state flow: 1, 3) approximation of a prescribed intensity; 2, 4, 5) account for self-defocusing; 1, 2) maximum velocity in the liquid; 3, 4) temperature on the axis at $z = 0.5\ H$; 5) angular divergence of the radiation beam that passed through the liquid, $\theta = 2w \cdot 57^0/H$; the points are experimental values. P_0, W.

a round cross section of the cell in the calculation region for the rectangular one in the experiments [1, 2], with the approximate correspondence of the taken boundary conditions to those of the experiment, and with experimental errors of measuring velocity and especially temperature.

Processing the results of the numerical modeling enabled us to determine the dependences of temperature and velocity in different cross sections z on the regime parameters of self-defocusing and convection. It was found that these dependences are not universal and vary with increasing z due to self-defocusing of radiation. For example, for PMS-20 liquid the dependence of the temperature T on the power P_0 varies as z increases and can be considered a power one, $T \sim P_0^n$, only in a specified and relatively small (narrow) interval of variation of P_0 (Fig. 4). In the range $P_0 = 13-74$ W at the center of the calculation region ($z = 0.5\ H$) the exponent $n_T = 0.36$ and coincides with that experimentally determined in [1, 2]. In the same range of power variation the exponent n_T varied from 0.32 at $z = 0.2\ H$ to 0.49 at $z = 0.8\ H$. The temperature of the liquid on the beam axis with account for self-defocusing and with no account for it is shown in Fig. 4. Self-defocusing leads to a decrease in the actual excess temperature by nearly an order of magnitude compared to the temperature that is obtained in the approximation of the prescribed intensity. A similar analysis was performed for the flow velocity on the beam axis. For PMS-20 with $P_0 = 13-74$ W the power approximation $u \sim P_0^{n_u}$ with $n_u = 0.4$ is practically unchanged in all the cross sections $z/H = 0-1$ if $\alpha H \lesssim 0.3$. For PES-4 liquid, which absorbs radiation relatively more strongly, where $\alpha H = 1$, the exponent n_u varies from 0.34 at $z = 0.2\ H$ to 0.46 at $z = 0.8\ H$. At $z = 0.5\ H$ we can take $n_u = 0.42$ for both liquids. This result does not contradict the experimental data [1, 2], where n_u increased with increasing z from 0.25 to 0.61 for PES-4 and from 0.4 to 0.63 for PMS-20. In root-mean-square processing of all regimes accounting for differences in the optical thickness αH the authors of [1, 2] obtained the value $\bar{n}_u = 0.5$ for three different liquids. The effect of self-defocusing on velocity manifests itself to a much smaller extent than on temperature (Fig. 4).

The dependence of the velocity on the beam axis $u(r = 0)$ on the vertical coordinate z can only approximately be considered to be a power one $u \sim z^{n_z}$ with exponent $n_z = 0.65-0.85$ for $P_0 = 13-74$ W and $n_z \approx 1$ for larger values of the power, which indicates a substantial effect of the zone of reverse motions in the vicinity of the cell walls, i.e., circulation flow in a closed cavity. A similar dependence of velocity on the coordinate also occurs in the prescribed-intensity approximation.

The numerical experiments showed that the thermal and hydrodynamic conditions on the upper boundary of the liquid (substituting an adiabatically insulated boundary for an isothermal one and substituting a solid wall for a free surface) have a weak effect on the character of u and T as functions of the power and a marked effect on u and T as functions of z.

An important parameter is the divergence of the radiation beam w as a function of the thermooptical interaction regime. Figure 4 shows the dependence $w(P_0)$, from which the applicability of the approximation $w \sim P_0^{n_w}$ with $n_w = 0.1$ follows, which is in agreement with the experimental data. A change in the character of the dependence $w(P_0)$ for $P_0 \gtrsim 70$ W is noteworthy. The calculations showed that the contribution of the initial divergence of the beam and diffraction divergence is additive for the parameters taken and is summed with the self-defocusing of the beam. It is also noteworthy that with a convective mechanism of self-defocusing the divergence of the beam and its dependence on the radiation power turn out to be much weaker than in the self-defocusing by heat conduction that is described in [4] (see [12, 13] for a discussion of this fact and the accompanying change in the radiation coherence).

Thus, accounting for self-defocusing leads to a lack of stabilization of the flow in the channel in both velocity and temperature in connection with a lack of stabilization of the radiation intensity. Therefore, the limiting regime of stabilization assumed in [5] is in fact not realized.

5. Comparing the results of numerical modeling with those of the dimensional analysis in Sec. 3 shows that the dimensional analysis yields a very incomplete and not always correct picture of thermooptical interaction both with account for self-defocusing and ignoring it. The dimensional estimates of T, w, and τ as functions of P_0 agree with the results of the numerical analysis quantitatively. However, the dimensional estimates of u as a functions of P_0 and ε_T are only in qualitative agreement with the actual situation. It is pertinent to note that the upper boundary of the regime of moderate convection is at least four orders of magnitude higher than the estimate of the dimensional analysis, which coincides with the conclusion of the authors of [9] obtained in the approximation of a prescribed intensity.

CONCLUSIONS

Taking account of self-defocusing of radiation alters qualitatively and quantitatively the features of light-induced convection and divergence of a beam in both the transient and steady-state phases of thermooptical interaction compared to the prescribed-intensity approximation. This difference is especially noticeable in the divergence of the beam (an increase in width of up to 500%) and the temperature of the liquid on the beam axis (a decrease of up to 500%).

Thermal self-defocusing extends markedly the time for establishing convection $\tau \sim I_0^{-0.31}$ compared to the approximation of a prescribed intensity, where $\tau \sim I_0^{-0.5}$. Self-defocusing leads to the impossibility of formation of a section of flow stabilization in the channel and to nonequivalent propagation of radiation from the bottom upward and from the top downward.

The effect of the boundary conditions as to temperature and velocity on the horizontal portion of the boundary of the liquid surface is smoothed out at a distance of about a cell diameter and they hardly affect the character of the velocity, temperature, and divergence of the beam as functions of the power. Due to the multiparameter nature of the problem, only in individual parameters do the results of dimensional analysis, agree with correlation dependences obtained as a result of physical and numerical experiments, and they are not universal, which manifests itself especially distinctly as the optical thickness of the liquid layer is varied.

The authors express their thanks to V. I. Zuev for discussing the experiments and for his kind permission to use his works [1, 2].

NOTATION

u, v, velocity; T, temperature; p, pressure; P, power; t, τ, time; z, r, vertical and radial coordinates; R, H, radius and height of the cylinder; I, radiation intensity; s, addition to the eikonal of the flat wave; k, modulus of

the radiation wave vector; Λ_0, w, initial and current width of the beam; θ, angular divergence of the beam; g, acceleration of gravity; β, ν, χ, κ, α, coefficients of thermal expansion, kinematic viscosity, thermal diffusivity, thermal conductivity, and radiation absorption; ρ, density; C_p, thermal capacity; ε, ε_T, dielectric permittivity and its thermal coefficient; $\bar{\varepsilon}_T$, thermal parameter of refraction; $\bar{\varepsilon}_T = \varepsilon_T \alpha I_0 \Lambda_0^2 / \varepsilon_0 \kappa$; Gr, Pr, Grashof and Prandtl numbers; $\mathrm{Gr} = g\beta\alpha I_0 \Lambda_0^5 \chi / \nu^3 \kappa$, $\mathrm{Pr} = \nu/\chi$.

REFERENCES

1. A. S. Gurvich and V. I. Zuev, "Experimental investigation of convection induced by powerful laser radiation," Moscow (1987) (Preprint IFA Akad. Nauk SSSR).
2. V. I. Zuev, "Experimental investigation of convection induced by powerful laser radiation (a vertical beam)," Candidate's Dissertation in Physicomathematical Sciences, Moscow (1988).
3. W. G. Wagner and J. H. Marburger, Opt. Commun., 3, No. 1, 19-20 (1971).
4. V. A. Aleshkevich, A. V. Migulin, A. P. Sukhorukov, et al., Zh. Éksp. Teor. Fiz., 62, No. 2, 551-561 (1972).
5. C. M. Vest, Phys. Fluids, 17, No. 11, 1945-1950 (1974).
6. S. H. Lehnigk and B. Steverding, J. Fluid Mech., 66, No. 4, 817-829 (1974).
7. A. V. Luikov and B. M. Berkovskii, Convection and Thermal Waves [in Russian], Moscow (1974).
8. B. P. Gerasimov, V. N. Gordienko, and A. P. Sukhorukov, "On free convection in photoabsorption," Moscow (1974) (Preprint, IPM Akad. Nauk SSSR, No. 59).
9. B. P. Gerasimov, V. N. Gordienko, A. P. Sukhorukov, et al., "Numerical investigation of photoabsorbing convection in a vertical cylindrical tube," Moscow (1976) (Preprint, IPM Akad. Nauk SSSR, No. 63).
10. J. P. Shuster, W. O. Li, and W. J. McLean, AIAA Paper, No. 1522 (1980).
11. W. P. Horn, M. S. Sheldon, and P. S. Boer, J. Phys. Chem., 90, No. 11, 2541-2548 (1986).
12. N. Ye. Galich and O. G. Martynenko, Heat Transfer, Sov. Res., 22, No. 4, 542-566 (1990).
13. N. Ye. Galich and O. G. Martynenko, "Optical turbulence and self-defocusing of a vertical radiation beam in a liquid or a gas in light-induced convection," Minsk (1991) (Preprint, ITMO Akad. Nauk BSSR, No. 20).
14. A. N. Bogaturov, V. I. Zuev, and V. M. Ol'khov, Zh. Éksp. Teor. Fiz., 94, No. 8, 152-165 (1988).
15. N. Ye. Galich, Zh. Tekh. Fiz., 55, No. 8, 1473-1481 (1985).
16. V. Steverding, Appl. Phys., 46, No. 9, 3906-3908 (1975).
17. O. G. Martynenko, Yu. A. Sokovishin, and Yu. E. Karyakin, "Free convection on a vertical surface and in arbitrarily shaped regions," Minsk (1988) (Preprint, ITMO Akad. Nauk BSSR, No. 3).
18. N. Ye. Galich and V. A. Petrushchenkov, Heat and Mass Transfer MMF-2, Abstracts of Papers [in Russian], Minsk (1992), Vol. 9, Part 2, pp. 37-39.
19. P. I.-Wu. Shen, P. A. Iyer, and D. R. Regan, J. Physique (coll.), 41, No. 1, C9-137–C9-147 (1980).